Astron. Astrophys. 184, 164–172 (1987)

ASTRONOMY AND ASTROPHYSICS

Evolution of stellar binaries formed by tidal capture

A. Ray, A.K. Kembhavi, and H.M. Antia

Tata Institute of Fundamental Research, Homi Bhabha Road, Bombay 400005, India

Received December 18, 1986; accepted March 20, 1987

Summary. Two-body tidal capture, as proposed by Fabian et al., is the favoured mechanism for the formation of X-ray binaries in globular clusters. We consider here the tidal capture formation and subsequent evolution of a system consisting of a neutron star and a low mass main sequence star. We obtain the amount of tidal energy deposited during the first and later close passages, and the radial distribution of this energy. Going further, we examine the effects of the viscous dissipation of the tidal energy on the structure of the low-mass star and on the binary system. The tidal energy is thermalized on a timescale of 10^4 yr. The consequent high tidal luminosity causes the star to expand and overflow its Roche lobe, resulting in the formation of a common envelope. This makes the stellar core and the neutron star spiral towards each other because of the frictional drag. The state reached by the system after the dissipation of the tidal energy depends on the relative values of the various timescales relevant to the system. Depending on these values the system may evolve into any of the following configurations: an X-ray binary, a detached binary, a neutron star surrounded by a massive accretion disk and a cloud of matter, or a Thorne-Zytkow object.

Key words: stars: evolution of – stars: binaries: close – stars: dynamics – clusters: globular – X-rays: binaries

1. Introduction

Globular clusters are known to be particularly fertile grounds for the formation of X-ray sources: the 134 known clusters in our galaxy contain at least 10 bright X-ray sources with $L_x > 10^{36}\,\mathrm{erg\,s^{-1}}$ (see Grindlay, 1985; Hertz and Wood, 1985, for a review). Approximately 10% of all known bright sources in the Galaxy are thus associated with $\sim 10^{-4}$ of the mass, as was first pointed out by Gursky (1973) and later by Katz (1975). The nature of the X-ray sources in globular clusters has not been observationally established, but there are several independent lines of evidence to suggest that these are close binary systems in which mass flows from a Roche-lobe filling star onto a neutron star companion (see Lightman and Grindlay 1982 for a discussion).

It was suggested by Clark (1975) that X-ray binaries in globular clusters are formed by the capture of a field star by a neutron star, rather than by the evolution of primordial binaries, because of the great age of the clusters. However, the cross-sections for the usual three-body processes which might lead to such capture are too small to be of interest. A novel method for the formation of X-ray binaries was suggested by Fabian et al. (1975). This process involves a close encounter between a neutron star and a non-collapsed ("normal") star. The encounter is such that tidal oscillations set up in the normal star take up sufficient energy to make the orbital energy of the system negative, leading to the formation of a bound system. The binary formed is necessarily a very close one, for otherwise the energy lost to the tides would not be sufficient to cause binding. Roche-lobe overflow by the normal star on to the condensed star can then commence to power an X-ray source. The number of such encounters expected in the dense cores of globular clusters is sufficient to explain the observed number of X-ray binaries found there.

The two-body tidal capture mechanism was investigated in detail by Press and Teukolsky (1977, hereafter PT). These authors have provided a formalism for calculating, in the linear approximation, the amount of energy deposited into oscillatory modes during a close periastron passage. The energy can be obtained in terms of dimensionless functions, independent of the mass or radius of the stars involved, but dependent on the envelope structure of the star. The numerical results presented by PT are applicable only to the case where the field star may be represented by a $n = 3$ polytrope.

We intend to investigate in this article the effect of the tidal energy deposited in the first and subsequent encounters on the structure of the normal star. The total amount of energy which could be deposited in the tides is $\sim GM_*M_n/R_{min}$ where M_* is the mass of the normal star and $R_{min} \sim 3R_*$ is the periastron distance required for capture. We will show in the following sections that, with the appropriate viscous dissipation timescale a "tidal luminosity" as high as $\sim 10^3$ times the luminosity of the star in the unperturbed state may be generated. This can have serious consequences on the evolution of the binary system, possibly preventing it from becoming an X-ray source, or even leading to the complete disruption of the normal star.

In the present work (1) we will use the formalism of PT to obtain tidal energy deposition and capture cross-section for a first encounter between a neutron star and a main sequence star, represented either by a $n = 3$ or a $n = 1.5$ polytrope. The typical low mass star in a globular cluster would tend to be fully convective and is more appropriately represented by the latter. It will be seen that the results for the two cases are significantly different.

Send offprint requests to: A. Ray

For the $n = 3$ case we will correct a numerical error in the reported calculation of PT. We will also use the formalism to estimate the energy deposited in the tides in successive periastron passages after the capture. (2) We will obtain the distribution of tidal energy as a function of stellar radius. This was not done by PT, but is useful for our purposes. (3) We will estimate the viscous dissipation timescale for the fully convective non-degenerate star and thereby the tidal luminosity, and (4) examine the consequences of the luminosity to the star and the binary system.

These latter processes have until recently not been considered in the literature; it has only been assumed that at some time after the formation, the system evolves into a low mass X-ray binary. Preliminary results on the type of system we consider have been reported by Antia, et al. (1986). McMillan et al. (1986) have considered the effects of tidal energy dissipation on a binary system consisting of two normal stars. They however use radiative dissipation in estimating damping timescales, which is appropriate for the stellar masses in their system. These authors do not consider the evolutionary scenarios for the binary in the way that we do here for stellar pairs consisting of a degenerate and a low-mass nondegenerate star.

The mathematical formalism we require will be described in Sect. 2. In Sect. 3 we will obtain numerical values for the tidal energy after the first passage, the capture cross section, and the tidal energy deposited in subsequent passages. The distribution of tidal energy inside the star will be obtained in Sect. 4. In Sect. 5 we obtain the viscous dissipation timescale appropriate to the problem, while in Sect. 6 we consider the response of the star to thermal dissipation. Finally, in Sects. 7 and 8 the evolution of the binary system and conclusions are presented.

2. The formalism

In the encounter between a neutron star and a normal star, the rate at which tidal energy is deposited in the latter is (PT 1)[1]

$$\frac{dE}{dt} = \int d^3x \rho \boldsymbol{v} \cdot \nabla U \tag{1}$$

where ρ is the density and $\boldsymbol{v}$ is the velocity of a fluid element in it: U is the gravitational potential of the neutron star, which is imagined to be a point mass:

$$U(\boldsymbol{r}, t) = \frac{GM_n}{|\boldsymbol{r} - \boldsymbol{R}(t)|} \tag{2}$$

Here M_n is the mass of the neutron star and the vector $\boldsymbol{R}(t)$ describes its orbit. At very large separations, the relative velocity of the two stars may be taken to be the average dispersion velocity of stars in the globular cluster, which is $\sim 10\,\mathrm{km\,s^{-1}}$. This is very small compared to their relative velocity at periastron, which can be several hundreds of $\mathrm{km\,s^{-1}}$. The eccentricity of the orbit will therefore be close to unity, and the orbit may very well be approximated as parabolic. Parametric equations for a parabolic orbit are quoted in PT 19–21[1].

[1] Equations from Press and Teukolsky (1977) will be cited as numbers following the letters PT.

The velocity $\boldsymbol{v}$ of a fluid element can be expressed in terms of its Lagrangian displacements $\boldsymbol{\xi}$ as

$$\boldsymbol{v} = \frac{\partial \boldsymbol{\xi}}{\partial t} \tag{3}$$

Assuming that the effect of ∇U on the static unperturbed star can be described by linearized perturbation analysis, the Fourier transform $\tilde{\boldsymbol{\xi}}$ of $\boldsymbol{\xi}$ may be analyzed into normal modes $\tilde{\boldsymbol{\xi}}_n$. These satisfy a linear self-adjoint eigenvalue equation (Chandrasekhar, 1964), and are taken to be orthonormal with weight ρ;

$$\int d^3x \rho \tilde{\boldsymbol{\xi}}_n \cdot \tilde{\boldsymbol{\xi}}_m = \delta_{nm} \tag{4}$$

A given normal mode of a spherical star may be written as the sum of radial and poloidal parts (PT 32; see Cox, 1980 for details):

$$\boldsymbol{\xi}_n(\boldsymbol{r}) \equiv \boldsymbol{\xi}_{nlm}(\boldsymbol{r}) = [\xi^R_{nl}(r)\hat{\boldsymbol{e}}_r + \xi^S_{nl}(r) r \nabla] Y_{lm}(\theta, \phi). \tag{5}$$

Here $\hat{\boldsymbol{e}}_r$ is a unit vector in the direction of $\boldsymbol{r}$ and $Y_{lm}(\theta, \phi)$ are spherical harmonic functions as in Jackson (1975).

The total energy transferred to the tides during the encounter can be expressed as

$$E_{\mathrm{tide}} = \int \frac{dE}{dt} dt = \frac{GM_*^2}{R_*} \frac{M_n^2}{M_*^2} \sum_{l=2}^{\infty} \left(\frac{R_*}{R_{\min}}\right)^{2l+2} T_l(\eta) \tag{6}$$

where M_* and R_* are the mass and radius respectively of the normal star, and the dimensionless variable η is defined by

$$\eta = \left(\frac{M_*}{M_* + M_n}\right)^{1/2} \left(\frac{R_{\min}}{R_*}\right)^{3/2} \tag{7}$$

with $R_{\min}$ the minimum distance of the approach. The quantity $\eta \sim t_p/t_h$, where $t_p \sim R_{\min}/v_p$ is the timescale for periastron passage with v_p the velocity at periastron, and $t_h \sim R_*/c_s$ is the hydrodynamic timescale of the star, with c_s the sound velocity. The dimensionless function $T_l(\eta)$ is defined as

$$T_l(\eta) = 2\pi^2 \sum_n |Q_{nl}|^2 \sum_{m=-l}^{l} |K_{nlm}|^2 \tag{8}$$

Here the dimensionless function Q_{nl} involves only the radial dependence of the eigenfunctions and the matter density:

$$Q_{nl} = \int_0^1 dr' r'^2 \rho'(r') l r'^{l-1} [\xi^R_{nl} + (l+1)\xi^S_{nl}] \tag{9}$$

where r' and ρ' are the radial coordinate and density expressed in units of R_* and M_*/R^{*3} respectively. The functions K_{nlm} involve only the eigenfrequencies ω_n and the time development of the trajectory. The expression for a parabolic trajectory is

$$K_{nlm} = \frac{W_{lm}}{2\pi} 2^{3/2} \eta I_{lm}(\eta \omega_n) \tag{10}$$

where

$$I_{lm}(y) = \int_0^{\infty} dx (1 + x^2)^{-l} \cos[2^{1/2} y (x + x^2/3) + 2m \tan^{-1} x] \tag{11}$$

and

$$W_{lm} = (-)^{(l+m)/2} \left[\frac{4\pi}{2l+1} (l-m)!\,(l+m)!\right]^{1/2} \Bigg/ \left[2^l \left(\frac{l-m}{2}\right)! \left(\frac{l+m}{2}\right)!\right] \tag{12}$$

where the symbol $(-)^k$ is to be interpreted as zero when k is not an integer. A numerical scheme for evaluating the function $I_{lm}(y)$ using rational function approximations has been given by PT.

The functions $T_l(\eta)$ can be obtained without reference to the masses and radii of the stars involved, or the minimum distance of approach. The energy transferred to the tides in specific cases can then be obtained from Eq. (6), and the cross-section for the formation of a binary determined, as explained in the next section.

3. Results for $n = 3$ and $n = 1.5$ polytropes

We have computed the eigenmodes of oscillation for $n = 3$ and $n = 1.5$ polytropes by solving the equations of linear adiabatic oscillations (cf. Unno et al., 1979, p. 134) using a finite difference method (Antia, 1979). We have considered only the $l = 2$ (quadrupole) tides. The $l = 0$ term contributes only an additive constant to the gravitational potential, while the $l = 1$ term makes a vanishing contribution to the tidal energy. The octupole ($l = 3$) term makes only a $\sim 10\%$ contribution, while the higher terms contribute $\leq 1\%$. We have neglected these higher moments since they are not important for our considerations. Results for the two cases are shown in Table 1, where we have tabulated eigenfrequencies and values of the corresponding functions Q_{nl}, for $l = 2$.

For the $n = 3$ polytrope, we have tabulated 19 p, f and g modes. Our frequencies which are in units of $(GM_*/R_*^3)^{1/2}$ agree well with those of PT (note that we list the value of ω_n^2 for each mode, while PT list $4\omega_n^2/3$). Our values of Q_{nl} are significantly lower than those of PT for $l = 2$, as well as for the $l = 3$ case, which we have computed, but not included in the present publication. We trace this discrepancy to an erroneous inclusion of an extra factor l, by PT in the second term on the right hand side of their Eq. 36 in their computation (note that equation PT 36 itself is correct). We are able to reproduce the values of Q_{nl} of PT by including this extra (erroneous) factor in our code. Recently Giersz (1986), Lee and Ostriker (1986), and McMillan et al. (1986), have also independently obtained some of the results reported in this section. These authors too have noticed the error in the results of PT, but have not traced it to the source.

For the $n = 1.5$ polytrope, we have included five p modes and the f mode. In this case, since the star is advectively neutral, there are no g modes, and hence there is no eigenfrequency lower than that of the f mode. The values of Q_{nl} are negligibly small for modes higher than p_5. The $|Q_{nl}|$ value for the f mode is an order of magnitude or more than that for the other modes, and the f mode makes the dominant contribution to the tidal energy.

The function $T_l(\eta)$ for the two polytropes is shown in Fig. 1. We have obtained the tidal energy $E_{\rm tide}$ from the $T_l(\eta)$ for the special case of parameter values: stellar mass $M_* = 0.6\,M_\odot$, neutron star mass $M_{\rm n} = 1.4\,M_\odot$ and dispersion velocity in the globular cluster, $v_{\rm d} = 10\,{\rm km/s}^{-1}$. We will always use these special values for the purpose of illustration. The radius of the normal star is assumed to be proportional to its mass, with the normalization $R_* = 4.5\,10^{10}$ cm for $M_* = 0.6\,M_\odot$ (cf. Allen, 1973, p. 209). $E_{\rm tide}$ as a function of the periastron distance $R_{\rm min}$ is shown in Fig. 2. The relative kinetic energy of the two stars for very large separations is $E_{\rm kin} = 4.2\,10^{44}$ erg in the special case. This value is marked on the tidal energy curves in Fig. 2. For values of $R_{\rm min}$ which are such that $E_{\rm tide} > E_{\rm kin}$, the relative orbital energy becomes negative after the encounter, and the system becomes gravitationally bound. The eccentricity immediately after the binding is very close to unity, and the orbital period is relatively large. A plot of the period after the first encounter against the closest distance of approach is also shown in Fig. 2.

Table 1. Eigenfrequencies and the functions Q_{nl} for $l = 2$

$n = 3$			$n = 1.5$		
Mode	ω_n^2	$\lvert Q_{nl}\rvert$	Mode	ω_n^2	$\lvert Q_{nl}\rvert$
p_4	59.41	0.02115	p_5	89.89	0.0002500
p_3	41.46	0.03503	p_4	63.46	0.0005663
p_2	26.72	0.06168	p_3	41.30	0.002525
p_1	15.26	0.1227	p_2	23.51	0.01058
f	8.174	0.2372	p_1	10.29	0.05580
g_1	4.915	0.09948	f	2.119	0.4909
g_2	2.828	0.04456			
g_3	1.822	0.02470			
g_4	1.270	0.01491			
g_5	0.9361	0.009439			
g_6	0.7185	0.006173			
g_7	0.5690	0.004097			
g_8	0.4618	0.002792			
g_9	0.3824	0.001889			
g_{10}	0.3218	0.001300			
g_{11}	0.2746	0.0009009			
g_{12}	0.2371	0.0006199			
g_{13}	0.2068	0.0004286			
g_{14}	0.1819	0.0003029			

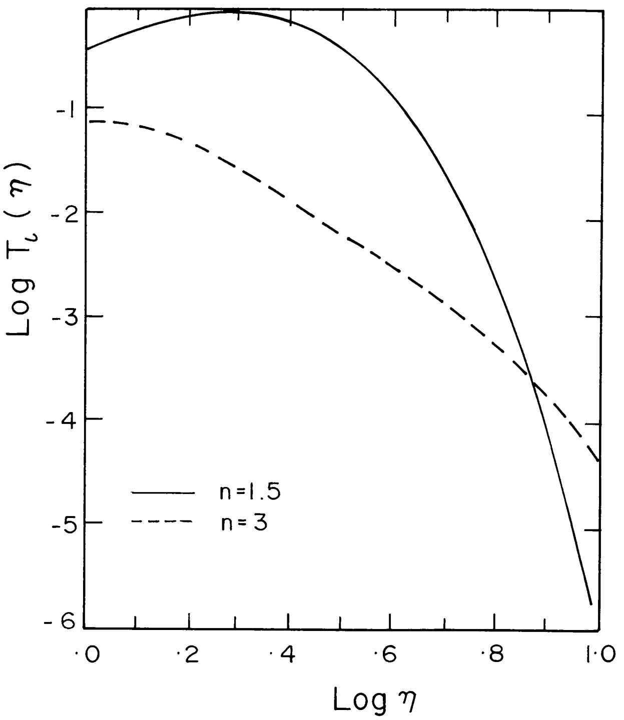

Fig. 1. The function $T_l(\eta)$ for $l = 2$. The polytropic index corresponding to each curve is indicated in the diagram

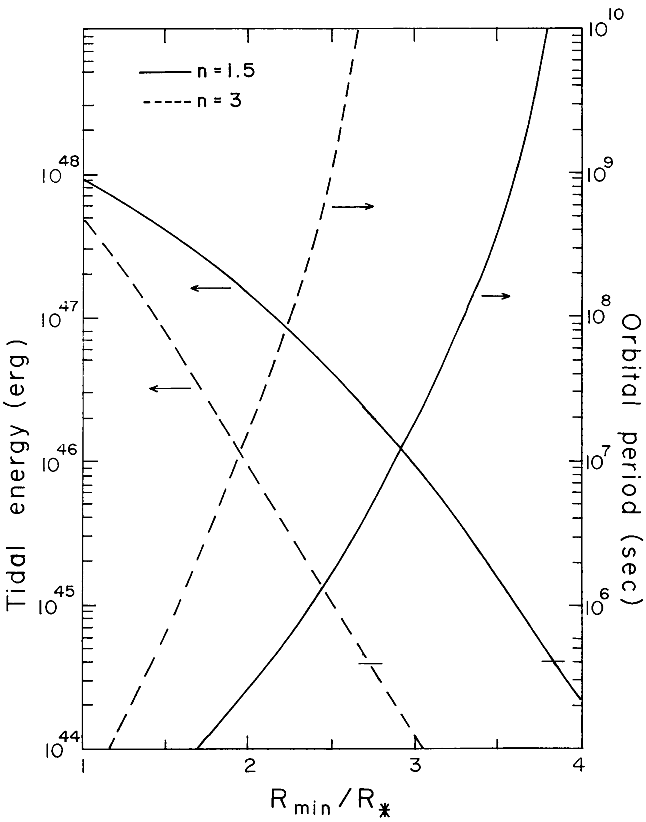

Fig. 2. Tidal energy and orbital period after the first periastron passage. The arrows indicate relevant axes. The notches on the energy curves indicate kinetic energy at infinite separation

The maximum periastron distance allowed, if capture is to take place in an encounter, as a function of M_* can be obtained by solving the equation

$$E_{orb} = E_{kin} - E_{tide} = 0 \tag{13}$$

for R_{min}. For values of R_{min} greater than such a value no capture is possible since sufficient energy is not dissipated in the tides. For a given capture radius, the capture cross-section is

$$\sigma = \pi R_0^2 \tag{14}$$

where the impact parameter R_0 is given by

$$R_0 = R_{min}\left[1 + \frac{2GM_T}{R_{min}\, v_d^2}\right]^{1/2} \tag{15}$$

with $M_T = M_* + M_n$ the total mass of the system. Since $v_d^2 \ll GM_T/R_{min}$, in effect $R_0 \propto R_{min}^{1/2}$; i.e., because of the gravitational focusing, $\sigma \propto R_{min}$.

We have shown in Fig. 3 the maximum periastron distance for capture as a function of stellar mass. The values assumed for the other parameters required in the calculation are the special values mentioned above. However, the maximum periastron distances obtained from Eq. (13) are weakly dependent on the values of the parameters; for instance, doubling the dispersion velocity would decrease R_{min} by $\sim 10\%$. Figure 3 can be used to directly estimate the cross-section for binary formation for stars of a given mass. For $M_* = 0.6\, M_\odot$, the capture cross-section for the $n = 1.5$ polytrope is larger than that for the $n = 3$ case by a factor close to 1.5. It can be noticed from Fig. 2 that for a given R_{min}, E_{tide} for $n = 1.5$ can be more than an order of magnitude larger than for $n = 3$. This allows capture at greater distance, proportionally increasing the cross-section. The collision rate per star $\Gamma = N\sigma v_d$ can be expressed as

$$\Gamma = 2.87\, 10^{-21}\left(\frac{M_T}{M_\odot}\right)\left(\frac{R_{min}}{R_*}\right)\left(\frac{R_*}{10^{10}\,\mathrm{cm}}\right)\left(\frac{v_d}{10\,\mathrm{km\,s^{-1}}}\right)^{-1}\left(\frac{N}{10^4\,\mathrm{pc^{-3}}}\right) \tag{16}$$

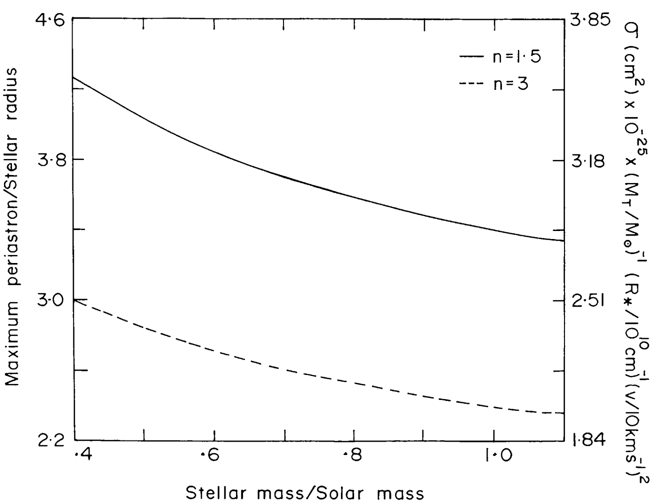

Fig. 3. Maximum periastron permitted for the first encounter, if capture is to be possible, as a function of the mass of the main sequence star. The cross-section for capture is also indicated

For the $n = 1.5$ polytrope it follows from Fig. 3 that the maximum periastron allowed for capture, for $M_* = 0.6\,M_\odot$, is $(R_{min}/R_*) = 3.84$. The collision rate for the usual parameter values is therefore $\Gamma = 9.9\,10^{-20}\,s^{-1}$. For $n = 3$, the maximum periastron is 2.72, and $\Gamma = 7.0\,10^{-20}\,s^{-1}$. For the encounter of two main sequence stars, which is the case considered by PT, the collision rates are $\Gamma = 5.14\,10^{-20}\,s^{-1}$ for $n = 1.5$ and $\Gamma = 3.67\,10^{-20}\,s^{-1}$ for $n = 3$. The last value is a factor ~ 2 lower than that obtained from Eq. (59) of Press and Teukolsky.

Once a bound system is formed, energy is deposited in the tides at every subsequent periastron passage until circularization of the orbit is achieved. The orbits are now elliptical, and the formalism of PT cannot, in principle be applied, since it is tailored to a parabolic orbit. But in the initial stages the orbits are highly eccentric, and since the tidal potential falls off very rapidly with increasing distance between the stars, Eq. (6) can still be used as a first approximation. We have obtained the tidal energy transferred in successive passages in this approximation, assuming that the orbital angular momentum remains constant (transfer of angular momentum to the tides and various other complications will be addressed in a future publication). For each orbit the orbital energy E_{orb} is obtained by subtracting the tidal energy excited in that passage from E_{orb} for the previous passage. The orbital parameters are then determined from the orbital angular momentum and energy. The maximum tidal energy which can be extracted from the system is $GM_*M_n/2\,R_{cir}$, where $R_{cir} = 2 \times$ (initial periastron distance R_{min}) is the radius of the circular orbit.

Accumulation of tidal energy for $n = 3$ and 1.5 polytropes are shown in Fig. 4. For $n = 3$ we have considered the evolution of an orbit with $R_{min} = 2.6\,R_*$ for the first passage. This is close to the maximum periastron permitted for capture. For $n = 1.5$, two cases are considered, one with $R_{min} = 3.7\,R_*$, again close to the limit for capture, and another with initial $R_{min} = 2.6\,R_*$. The values of various stellar parameters are as given previously. When the initial periastron is close to the maximum allowed, the orbit evolves rather gently, so that the eccentricity reduces to just ~ 0.7 in as many as a thousand passages. It is seen from Fig. 4 that the time taken to reach this stage is $4.4\,10^9$ s for $n = 1.5$ and $5.2\,10^9$ s for $n = 3$. In either case about half the available energy passes to the tides by this stage. When the initial periastron is well within the limit for capture, the orbit evolves more rapidly. For $R_{min} = 2.6\,R_*$ with $n = 1.5$, the eccentricity reduces to 0.77 in 10 passages and $\sim 40\%$ of the available energy passes to the tides. The time taken for the 10 passages is $6\,10^6$ s. In 50 orbits, which take $9\,10^6$ s, $\sim 75\%$ of the energy is extracted; but the eccentricity now reduces to 0.5, and the calculations are no longer sufficiently accurate. One can however safely state that in this case $\sim 2\,10^{47}$ erg accumulate in the quadrupole tides in $\sim 10^7$ s. The energy accumulated in the other two cases we have considered is of the same order of magnitude, though the time taken is $\sim 5\,10^9$ s.

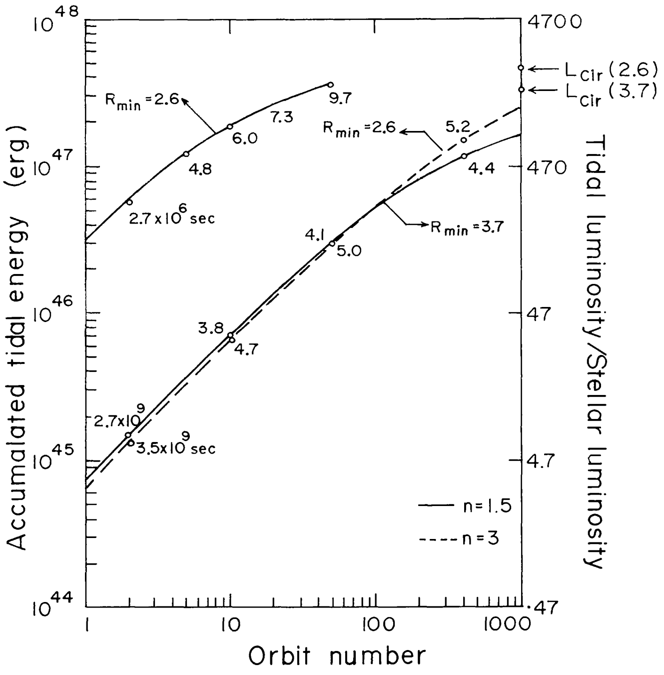

Fig. 4. Energy accumulated in the tides as a function of orbit number. Also shown is the corresponding luminosity for a viscous dissipation timescale of 10^4 yr. Indicated along each curve is the periastron distance R_{min} for the first passage, and the time spent in arriving at various orbits. The limiting luminosity L_{cir} for each value of R_{min} is indicated

4. Radial distribution of tidal energy

The distribution of tidal energy as a function of the stellar radius can be obtained using the formalism outlined in Sect. 2. From Eqs. (1) and (3) it follows that

$$\frac{dE_{tide}(\boldsymbol{r})}{dt\,dV} = \rho \boldsymbol{v} \cdot \nabla U = \rho \frac{\partial \boldsymbol{\xi}}{\partial t} \cdot \nabla U \tag{17}$$

where the expression on the left is the rate at which energy density accumulates at a given point in the star. The tidal energy density after the encounter is given by

$$\frac{dE_{tide}(\boldsymbol{r})}{dV} = \rho(\boldsymbol{r}) \int_{-\infty}^{+\infty} \frac{\partial \boldsymbol{\xi}}{\partial t} \cdot \nabla U\,dt \tag{18}$$

where we have neglected a higher order flux term. The expression on the right can be simplified by introducing the Fourier transforms $\tilde{\xi}$ and $\tilde{U}$ of ξ and U, respectively, analyzing these over normal modes, and integrating over time and frequency. Ultimately, the tidal energy density is expressed as

$$\frac{dE_{tide}}{dV}(\boldsymbol{r}) = 2\pi^2 \rho \sum_{n,n'} \tilde{\xi}_n \tilde{\xi}_{n'} A_n(\omega_n) A^*_{n'}(\omega_n) \tag{19}$$

where

$$A_n(\omega_n) = A_{nlm}(\omega_n) = \left(\frac{GM_n^2}{R_*}\right)^{1/2} \left(\frac{R_*}{R_{min}}\right)^{l+1} Q_{nl} K_{nlm} \tag{20}$$

We can now obtain the tidal energy density as a function of the radial coordinate r by averaging over the spherical shell of radius r, using the usual orthonormalization conditions on the spherical harmonics (see Jackson, 1975). Thus

$$\frac{\dfrac{dE_{tide}}{dV}}{\left\langle \dfrac{dE_{tide}}{dV} \right\rangle} = \frac{\rho' \sum_{nl} Q_{nl}^2 \left(\dfrac{R_*}{R_{min}}\right)^{2l+2} [(\xi_{nl}^{\prime R})^2 + l(l+1)(\xi_{nl}^{\prime S})^2] \sum_m |K_{nlm}|^2}{3 \sum_{nl} \left(\dfrac{R_*}{R_{min}}\right)^{2l+2} Q_{nl}^2 \sum_m |K_{nlm}|^2} \tag{21}$$

where the tidal energy density averaged over the whole star,

$$\left\langle \frac{dE_{\rm tide}}{dV} \right\rangle = \frac{E_{\rm tide}}{(4\pi/3)R_*^3} \tag{22}$$

has been introduced in order to make the right hand side dimensionless, $\xi'_{nl} = \xi_{nl} M_*^{1/2}$ and $\rho' = \rho(R_*^3/M_*)$. Here we have neglected cross terms in the summation since these will cancel out on integration over the whole volume. The tidal energy within a sphere of radius r is given by

$$\frac{E_{\rm tide}(<r)}{E_{\rm tide}} = \int_{r'=0}^{r/R_*} 3 \left\langle \frac{dE_{\rm tide}}{dV} \right\rangle^{-1} \frac{dE_{\rm tide}(r')}{dV} r'^2\, dr' \tag{23}$$

The distribution of energy density as a function of radius is shown in Fig. 5. The ordinate here is the integrand in Eq. (23), which is the energy density weighted by the area of a spherical shell of radius r. The solid lines indicate the energy distribution for the $n = 3$ polytrope for different values of the parameter η. As η increases, the peak of the distribution moves inwards, and the bulk of the tidal energy is deposited closer to the center of the star. The broken line indicates the energy distribution for the $n = 1.5$ polytrope. In this case, since the overwhelming contribution is by the f mode, there is a near cancellation of the η dependent terms in the numerator and denominator of Eq. (21), making the distribution quite independent of η. The energy distribution in the $n = 1.5$ case peaks away from the center, and the outer 30% of the mass of the star contains 60% of the tidal energy deposited.

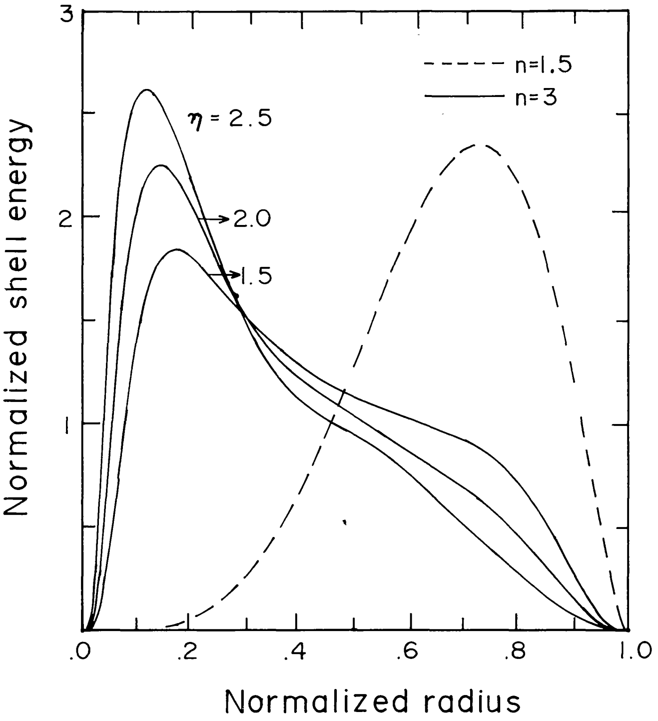

Fig. 5. The distribution of tidal energy as a function of radius, for various values of η. For the $\eta = 1.5$ polytrope the curves for the range of η values considered merge into each other

5. Viscous dissipation of tidal energy

The energy deposited in the star is initially in the form of the mechanical energy of the tidal oscillations. In Sect. 4 it is shown that for a $n = 1.5$ polytrope this energy is concentrated in the outer one third of the stellar radius, while for a $n = 3$ polytrope it is concentrated towards the center.

In a star with a substantial convective zone the most efficient damping mechanism would be due to the turbulent viscosity of convective eddies. For modes which are restricted to the inner radiative region, the damping will be due to radiative conductivity, which is less efficient. We will be concerned with stars of low mass (our detailed calculations are $M_* = 0.6\,M_\odot$), which are almost fully convective, where turbulent viscosity provides the damping. We have assumed in our calculations that the various oscillatory modes can be treated within the framework of linear perturbation theory. In reality however, because of large amplitudes of oscillation for captures which occurred in close collisions various nonlinear effects might be present, which may in fact reduce the damping time. Since there is no straightforward way to incorporate the nonlinear effects, we will restrict ourselves to the linear theory.

The timescale of viscous dissipation may be approximated by

$$\tau_{\rm visc} \simeq \frac{l^2}{\nu_{\rm eff}} \tag{24}$$

where l is the mixing length and $\nu_{\rm eff}$ is the effective turbulent viscosity in the convection zone. Normally, the turbulent viscosity ν_t is given by

$$\nu_t = l v_c \tag{25}$$

where v_c is the convective velocity which can be obtained from the usual mixing length theory. Neglecting factors of order unity, this is

$$v_c = [L/4\pi r^2 \rho]^{1/3} \tag{26}$$

where L is the stellar luminosity and ρ the density at radius r. However, as Goldreich and Keeley (1977) have pointed out, viscosity is less effective when the characteristic timescale of perturbation (here the oscillatory period) is shorter than the eddy turnover time (l/v_c). In that case $\nu_{\rm eff} = \nu_t/\beta^2$ where

$$\beta \simeq \frac{\omega_n}{2\pi} \frac{l}{v_c} \sqrt{\frac{GM_*}{R_*^3}} \tag{27}$$

with ω_n the oscillation frequency in units of $(GM/R^3)^{1/2}$ for the nth mode, M_* the stellar mass, and R_* the stellar radius.

Using the above equations and approximating ρ by the mean density, we get the viscous timescale

$$\tau_{\rm visc} = \frac{3\omega_n^2}{4\pi^2} \left(\frac{l}{R_*}\right)^3 \frac{GM_*^2}{R_* L_*} \tag{28}$$

We will now specialize to the case of a $n = 1.5$ polytrope, which is fully convective and therefore the relevant model, with mass $M_* = 0.6\,M_\odot$. In this case the f mode, for whch $\omega_n^2 = 2.1$, is the most dominant and an approximate expression for the viscous timescale is

$$\tau_{\rm visc} = 1.6\,10^7\,{\rm yr} \left(\frac{l}{R_*}\right)^3 \left(\frac{M_*}{0.6\,M_\odot}\right)^2 \left(\frac{R_*}{4.5\,10^{10}\,{\rm cm}}\right)^{-1} \left(\frac{L}{0.172\,L_\odot}\right)^{-1} \tag{29}$$

where we have normalized the radius and luminosity to values adequate for the stellar mass. Using $l/R_* \simeq 0.1$ we get $\tau_{\rm visc} \simeq 10^4$ years. Of course this estimation is very rough and could be off by an order of magnitude. But our results are not critically dependent on the values of this timescale, and we shall use $\sim 10^4$ years for it in subsequent calculations.

The viscous dissipation of tidal energy generates a luminosity which may be approximated by

$$L_{\rm tide} \simeq \frac{E_{\rm tide}}{\tau_{\rm visc}} \qquad (30)$$

where $E_{\rm tide}$ is the accumulated tidal energy. $L_{\rm tide}$ is shown as a function of orbit number in Fig. 5, for polytropes with $n = 1.5$ and $n = 3$: the values of $R_{\rm min}$, the distance of closest approach for the first encounter, are indicated alongside the curves. The maximum energy which can be extracted from the orbit is $E_{\rm cir} = GM_* M_n / 2 R_{\rm cir}$, where $R_{\rm cir}$ is radius of the orbit after circularization, assuming no mass is lost from the system. Values of $L_{\rm cir} = E_{\rm cir}/\tau_{\rm visc}$ for $\tau_{\rm visc} = 10^4$ yr, assuming constant mass and orbital angular momentum, are shown in Fig. 4. The time taken for circularization cannot be estimated within the present treatment, since the formalism used is not valid for eccentricity not close to unity, and there are several effects not taken into account here that would become important at small eccentricity. However, from the times of successive periastron passages (with $t = 0$ for the first passage) indicated in Fig. 4, it is clear that substantial luminosity is generated even for $t \ll \tau_{\rm visc}$. At such times the eccentricity is sufficiently large and the approximations used in the calculations are valid, unless the collision is much closer than what is maximally allowed. It is clear that the tidal luminosity roughly 1000 times the normal stellar luminosity may be generated and maintained over the viscous dissipation timescale. It should be noted here that $\tau_{\rm visc}$ is inversely proportional to the luminosity, so that as the star adjusts to the new luminosity, $\tau_{\rm visc}$ will decrease significantly. This feedback control will tend to increase the thermal luminosity, but this will operate on the (long) thermal (Kelvin Helmholtz) timescale.

6. Response of main sequence star to tidal luminosity

We have seen in the previous section that viscous dissipation of the accumulated tidal energy leads to a substantially enhanced luminosity in the "normal" star, which we will assume is on the main sequence. The star responds to this increased luminosity by attempting to achieve a new equilibrium configuration, which generally involves expansion of the star. We will now estimate how much this will be, first assuming that the energy is artificially deposited in an isolated star, and then consider the effect of the presence of the neutron star in a binary orbit.

To quantitatively assess the response of the star to the tidal luminosity, it would be necessary to numerically evolve a star using a stellar evolution code. We will defer this to a future publication, and provide here only a qualitative estimate, using the analytic treatment of Stein (1966, p. 23). It follows from the work of Stein that for Population II stars of low mass,

$$L_* \propto R_*^3 \qquad (31)$$

with L_* and R_* the luminosity and radius, respectively, of a star. This relation, though approximate, is sufficient to provide a rough estimate of the extent of the expansion. As will be seen later on, our conclusions to an extent do not depend critically on how far the star expands.

Since $L_{\rm tide} \simeq 1000$ times the normal luminosity, we can expect the star to expand to about 10 times its original radius. We can expect this to happen over the Kelvin-Helmholtz timescale $\tau_{\rm KH}$. Since $GM_*^2/R_* L_{\rm tide} \sim (4\text{–}6)$ in all cases, it follows that $\tau_{\rm KH} \simeq \tau_{\rm visc}$. Expansion of the star will therefore occur roughly over the viscous dissipation timescale. At the end of this period, the tidal energy would be spent, the tidal luminosity would decrease, and the star would contract back to its original size if it were an isolated object.

The simple picture of expansion and recontraction of the star is no longer applicable when it is part of a close binary system. In this case, expansion leads to loss of matter to the neutron star, the possible formation of a common envelope, and perhaps loss of matter from the system. We will consider these possibilities assuming that the binary system can be described in terms of simple Roche geometry. This is strictly true only when the orbit is circularized, and the rotation of the stars is synchronized with the orbital motion. We will nevertheless use the concept of Roche lobes as a first approximation, relying on the fact that the eccentricity rapidly decreases towards zero.

The radius $R_{\rm c}$ of the Roche critical surface surrounding the main sequence star is given by (Paczynski, 1971)

$$\frac{R_{\rm c}}{R_{\rm orb}} = 0.462 \left(\frac{M_*}{M_{\rm T}}\right)^{1/3} \qquad (32)$$

where $M_{\rm T} = M_{\rm n} + M_*$ is the total mass and $R_{\rm orb}$ the orbital separation. The above relation is valid when $M_*/M_{\rm n} \leq 0.8$, which is true in our case. Under the assumption of constant orbital angular momentum, the radius of the final circular orbit is $2\,R_{\rm min}$. For $R_{\rm min} = 2.6\,R_*$, which is the special case we will consider, $R_{\rm c} = 1.6\,R_*$. The Roche lobe is therefore close to the surface of the star, and well before the stellar radius expands to the value derived from (31), it overruns the critical surface. Some of the overflowing matter will be accreted onto the neutron star, while the rest of it will form a common envelope inside which the main sequence star as well as the neutron star move. Some of the matter in the common envelope could be lost through the outer Lagrangian points.

7. Evolution of the binary system with a common envelope

The effect of the frictional drag due to the common envelope on the neutron star, or on dense stellar cores, has been discussed by many authors in different contexts (e.g., Paczynski, 1976; Taam et al., 1978; Meyer and Meyer-Hofmeister, 1979). Following the treatment of Paczynski (1976), the rate of energy dissipation due to the frictional drag on the neutron star can be estimated to be

$$\dot{E} = \pi\, R_{\rm A}^2\, \rho v^3 \,, \qquad (33)$$

where ρ is the density of the common envelope at the orbit of the neutron star, and v its velocity relative to the envelope; we will approximate v by the orbital velocity $(GM_{\rm T}/R_{\rm orb})^{1/2}$ and the extent of the envelope roughly by that of the orbital dimensions of the binary. In Eq. (33) $R_{\rm A}$ is the accretion radius of the neutron star,

$$R_{\rm A} = \frac{GM_{\rm n}}{v^2 + c_{\rm s}^2} \qquad (34)$$

where c_s is the sound speed. In general $c_s \ll v$, and can be neglected. A similar drag acts on the dense portion of the companion star because of its motion in the common envelope. As a result of this the stellar core and neutron star spiral towards each other. The energy dissipated due to the friction comes from the orbital energy, so that the spiralling-in timescale is given by

$$\tau_{sp} \simeq \frac{R_{orb}}{\dot{R}_{orb}} = \frac{GM_* M_n}{R_{orb}\dot{E}} \tag{35}$$

The evolution of the binary system and its configuration after the stars have spiralled in towards each other, depends on how this timescale τ_{sp} compares with other relevant timescales. Firstly, the main sequence star overfills the Roche-lobe in an expanded state as long as the tidal oscillation energy is dissipated inside the star which is also roughly the thermal relaxation time. If the spiraling-in time τ_{sp} is very long due to low density in the common envelope compared to the dissipation timescale (τ_{visc}), then before any significant spiraling-in takes place the main sequence star would contract back inside the Roche-lobe and would no longer maintain a significant common envelope. In this case, a detached binary would result. On the other hand, if $\tau_{sp} \le \tau_{visc}$ the decay of the orbit would continue and in this case the final configuration depends on whether the dissipated energy is mostly radiated away from the surface or is used to eject matter from the common envelope. Following Taam et al. (1978) we will assume that if frictional heating is strong enough to heat matter in the envelope to escape velocity before the energy could be transmitted through, then the envelope will be ejected. If τ_{ej} is the time required to impart energy to the envelope by frictional heating equal to its binding energy, then,

$$\tau_{ej} = \frac{GM_T}{R_{env}\dot{E}} \Delta M_{env} \tag{36}$$

On the other hand, the time to transport energy across the envelope τ_{tr} (if this happens through convection) is:

$$\tau_{tr} \simeq \frac{l_{mix}}{v_{conv}} \simeq \frac{R_{orb}}{v_{orb}} \tag{37}$$

where $v_{conv} = [L/4\pi r^2 \rho]^{1/3}$, L being the luminosity going through the envelope. Thus, in the case $\tau_{sp} \le \tau_{visc}$, three distinct subclasses of final configurations might result. When $\tau_{ej} \gg \tau_{conv}$, the envelope of the main sequence star (which by now is in a bloated phase to fill the Roche-lobe) is not ejected and the neutron star spirals-in all the way to the center of the expanded star. In the final stage, the neutron star at the center of the other star generates an extremely high luminosity (limited only by the Eddington limit) due to gas accretion onto its surface. The resulting configuration of the system is similar to that investigated by Thorne and Zytkow (1977) and is a large red supergiant star.

If, on the other hand, $\tau_{ej} \le \tau_{conv}$ (with $\tau_{sp} \le \tau_{visc}$, as before), again two subclasses of final configurations may occur. The common envelope will be ejected entirely in these two different final configurations. In one case, the common envelope would be ejected faster than the rate at which the matter in it is replenished by Roche-lobe overflow after a while. This will result in a contact X-ray binary if the main sequence star just fills the Roche-lobe after the rapid orbit contraction (due to frictional drag in the common envelope) is over, due to decreased common envelope density. Due to differences in efficiency of viscous dissipation, the largest part of the tidally-induced thermal luminosity may come from very near the original stellar surface rather than deep down. Also, since the temperature at a given point decreases sharply with radius near the surface any extra heat deposition might change the entropy structure of the star dramatically towards the surface. This may shut off convection locally and might isolate the interior from the surface at least on thermal relaxation timescales. In such a case, the layers near the surface would expand and form the common envelope which in several episodes might then be ejected by the orbiting neutron star. Eventually, the interior which remained isolated from the surface due to entropy barriers, may fill the Roche-lobe and a contact X-ray binary may result, whose orbit will evolve only on mass-transfer timescales.

Alternatively (with $\tau_{ej} \ll \tau_{conv}$, and $\tau_{sp} \le \tau_{visc}$), the circumbinary envelope density may continue to remain high if much of the stellar mass participates in initial Roche-lobe overflow and in that case the neutron star spirals close to the center of the normal star and continues to eject the matter in the star due to release of orbital energy. In this case the final system could consist of a rapidly spinning neutron star surrounded by some matter, possibly in the form of a massive disk, with the rest of the matter ejected to infinity.

8. Conclusion

Two-body tidal capture and the subsequent evolution of a binary leads to the release of $\sim GM_* M_n/4R_{min} \sim 10^{48}$ erg to the tides excited in the main sequence star. The part of this energy located in the convection zone would be dissipated comparatively rapidly by turbulent eddies, while the energy in modes which are primarily restricted to the radiative region may not dissipate as efficiently. The viscous dissipation timescale relevant in the present context is $\tau_{visc} \sim 10^4$ years. For the $n = 1.5$ polytrope which approximates a fully convective star, this implies thermalization of the tidal energy at the rate $\sim 800\,L_\odot$. This energy is dissipated closer to the surface compared to the $n = 3$ case. For the $n = 3$ polytrope, the tidal energy resides in the g modes as well as the f and p modes. It is only the last two types of modes which exist in the convection zone, and the corresponding energy is thermalized on the viscous dissipation timescale. The fraction of energy in the f and p modes is a function of the parameter η (see Eq. (7)). For η values corresponding to $R_{min} = 2.6\,R_*$ to $R_{min} = 5.2\,R_*$, this fraction ranges from $\sim 20\%$ to less than 1%. Assuming a rough average of $\sim 10\%$, the thermalization of the tidal energy takes place at a rate $\sim 80\,L_\odot$. The energy in the g modes would be thermalized on timescales longer than τ_{visc}, unless non-linear mode couplings and other complications hasten the process.

The release of thermal energy at these rates can lead to the expansion of the main sequence star, which can have serious consequences for the binary. The main sequence star might rapidly overflow its Roche-lobe, which results in a common envelope around the binary system. The common envelope causes the stellar cores to spiral towards each other because of the frictional drag. The subsequent evolution depends on the ratio of spiral-in timescale to the viscous dissipation timescale, and also the ratio of the timescale for the ejection of the envelope to the timescale for the transport of thermal energy across the envelope. Depending on the circumstances the following scenarios are possible:

(1) If $\tau_{visc} < \tau_{sp}$, the common envelope formed is never of sufficient density to cause significant spiralling-in of the stars. After the tidal energy is dissipated, the system will evolve to a detached binary, consisting of a non-condensed star with mass

smaller than the original, and a neutron star. This may later evolve into an X-ray source over the nuclear evolution timescale of the "normal" star or due to orbit contraction owing to loss of angular momentum, e.g. through gravitational radiation.

(2) If $\tau_{visc} > \tau_{sp}$, there will be significant spiralling-in with a succession of envelope ejections. If the ejection of matter is efficient, after the exhaustion of the tidal energy which may be deposited close to the original surface of the star, a close binary system in which the non-condensed star just fills the Roche-lobe may be obtained. An X-ray source is thus immediately produced.

(3) If $\tau_{visc} > \tau_{sp}$, but the ejection is not efficient, the neutron star will spiral close to the center of the non-condensed star, which will be completely disrupted through a series of ejections. In this case we will be left with a neutron star surrounded by a massive disk, with much of the matter in the star dispersed to infinity. The neutron star could be spun up to very high rotational velocity due to angular momentum transfer from the disk.

(4) If $\tau_{visc} > \tau_{sp}$ and $\tau_{conv} < \tau_{ej}$, the neutron star will fall into the non-condensed star without ejecting much of the matter. In this case a Thorne-Zytkow supergiant is produced. However, the occurrence of the final configuration as a Thorne-Zytkow object is probably relatively rare.

It is generally believed that the X-ray sources in the cores of globular clusters are binaries formed by tidal capture. Our analysis shows that not all binaries formed by tidal capture need have evolved into X-ray sources within the time which has been available. It is not possible for us at the present to estimate the relative frequency with which an alternative, like (2) above, which does lead to an X-ray source, is realized in practice. If this does not happen sufficiently frequently, then some formation mechanism, other than two-body tidal capture, may be necessary to explain at least some of the globular cluster X-ray sources.

Acknowledgements. We wish to thank S.M. Chitre, E.P.J. van den Heuvel, Bruce Margon, Jayant Narlikar, Martin Rees, Malvin Ruderman, Bill Saslaw, and Ronald Webbink for discussions. One of us (AR) wishes to thank the Department of Astronomy at the University of Illinois and the University of Washington for assistance, and Commission 38 of the International Astronomical Union for partial travel support.

Note added in proof: A 3 ms pulsar has recently been discovered in the Globular Cluster M28 by Middleditch et al (IAU Circular No. 4401). This has a low upper limit of period derivative suggesting that it is not likely to be in a binary system. One of the possible ways to form such a system through tidal capture is outlined in Sections 7 and 8 (case (3)). In this case, the angular momentum stored initially in the disk can be transferred to the neutron star and eventually, a single fast pulsar will be left behind.

References

Allen, C.W.: 1973, *Astrophysical Quantities*, William Clowes, London
Antia, H.M.: 1979, *J. Comp. Phys.* **30**, 283
Antia, H.M., Kembhavi, A.K., Ray, A.: 1986, in *Globular cluster systems in Galaxies*, Proc. IAU Symp. No. **126**, D. Reidel, Dordrecht, (in press)
Chandrasekhar, S.: 1964, *Astrophys. J.* **139**, 664
Clark, G.W.: 1975, *Astrophys. J.* **139**, 664
Cox, J.P.: 1980 *Theory of Stellar Pulsation*, Princeton University Press
Fabian, A.C., Pringle, J.E., Rees, M.J.: 1975, *Monthly Notices Roy. Astron. Soc.* **172**, 15p
Giersz, M.: 1986, *Acta Astron.* **36**, 181
Goldreich, P., Keeley, D.A.: 1977, *Astrophys. J.* **211**, 934
Grindlay, J.E.: 1985, in *Compact Galactic and Extragalactic X-ray Sources*, eds. Y. Tanaka, W.H.G. Lewin, Institute of Space and Astronomical Science, Tokyo
Gursky, H.: 1973, in *Physics of Compact Objects*, NATO Advanced Study Institute, Cambridge, England
Hertz, P., Wood, K.S.: 1985, *Astrophys. J.* **290**, 171
Jackson, J.D.: 1975, *Classical Electrodynamics*, John Wiley, New York
Katz, J.I.: 1975, *Nature* **253**, 698
Lee, H.M., Ostriker, J.P.: 1986, *Astrophys. J.* **310**, 176
Lightman, A.P., Grindlay, J.E.: 1982, *Astrophys. J.* **262**, 145
McMillan, S.L.W., McDermott, P.N., Taam, R.E.: 1986, (preprint)
Meyer, F., Meyer-Hofmeister, E.: 1979, *Astron. Astrophys.* **43**, 309
Paczynski, B.: 1971, *Ann. Rev. Astron. Astrophys.* **9**, 183
Paczynski, B.: 1976, in *Structure and Evolution of Close Binary Systems*, eds. P. Eggleton, S. Mitton, J. Whelan, Reidel. Dordrecht p. 75
Press, W.H., Teukolsky, S.A.: 1977, *Astrophys. J.* **213**, 183 (PT)
Stein, R.F.: 1966, in *Stellar Evolution*, eds. R.F. Stein, A.G.W. Cameron, Plenum Press, New York
Taam, R.E., Bodenheimer, P., Ostriker, J.P.: 1978, *Astrophys. J.* **222**, 269
Thorne, K.S., Zytkow, A.N.: 1977, *Astrophys. J.* **212**, 832
Unno, W., Osaki, Y., Ando, H., Shibahashi, H.: 1979, *Nonradial Oscillations of Stars*, University of Tokyo Press